

Frequency renormalization and its effects in nonlinear phononics with $Q_R Q_{IR}^2$ -type coupling

Yijie Zeng*

College of Science, Hangzhou Dianzi University, Hangzhou 310018, China

(Dated: May 19, 2026)

A two-phonon system with lowest-order coupling of form $Q_R Q_{IR}^2$ is studied by perturbation method, and analytic results for both phonon displacements and frequencies are obtained. The frequency renormalization of infrared (IR) active mode brings the rectification of Raman mode to saturate at high pump field. For degenerate IR mode with coupling of form $Q_R(Q_{IR,x}^2 - Q_{IR,y}^2)$, the frequency of IR mode will split when resonantly pumped by elliptically or linearly polarized ultrashort mid-IR pulse, realizing Raman rectification and magnetization simultaneously. Our results reveal a dynamical effect of nonlinear phononics not captured by first-principles calculation, extend the dynamical multiferroicity to systems with coupling $Q_R(Q_{IR,x}^2 - Q_{IR,y}^2)$, and the method can be readily applied to higher-order couplings. The amplitude saturation under strong pump field stimulates future researches to overcome this nonlinear effect.

I. INTRODUCTION

In recent years, due to the development of high-intensity infrared (IR) laser pulses¹⁻³ and the computational efforts⁴⁻⁷ in revealing the anharmonic coupling between IR and other modes (e.g. Raman phonon, ferroelectric soft phonon mode⁸⁻¹⁰), nonlinear phonon coupling¹¹ was found to exist in a wide variety of materials, and plays an important role in light-induced superconductivity¹², light-induced magnetism (CoF₂)¹³, ultrafast switching of ferroelectricity^{14,15}, phonon-induced geometric chirality^{16,17} and multiferroic polarization¹⁸, etc. Compared with other static manipulation methods such as high-pressure, strain or heterostructure engineering, nonlinear phonon coupling is mode-selective, fast (within picoseconds), and often drives the system to a symmetry-breaking state which has no equilibrium counterpart¹⁹.

The physics behind nonlinear phononics is a nonvanishing cubic term $Q_R Q_{IR}^2$ in lattice potential, which couples IR active mode and Raman active (or silent) mode. Here Q_R/IR denote the normal coordinates of the coupled Raman active (or silent) and IR active mode, respectively. The irreducible representations of the coupled Q_R and Q_{IR} can be determined by requiring that $\Gamma_R \otimes \Gamma_{IR}^2$ contains the totally symmetric irreducible representation²⁰. When the IR active mode is resonantly pumped by laser pulse of form $F_0 e^{-t^2/\sigma^2} \cos(\omega_{IR}^{(0)} t)$, the Raman mode oscillates in $2\omega_{IR}$ around a displaced nonequilibrium position²¹, realizing rectification of Raman mode. Experimentally, the magnitude of rectification is found to scale with square of the electric field of pumped light^{13,17,22}, while it's not clear whether this behavior will survive under stronger laser pulses. Some theoretical works on HgTe¹⁹, Mott insulating titanites YTiO₃²³ and YBa₂Cu₃O₇²⁴ give hints that the rectification tends to saturate at high pump field, yet whether it is a general feature of cubic anharmonicity cannot be determined affirmatively. These facts arouse the interesting question — is it possible to drive the Raman mode to any desired rectified position with stronger pump pulse?

It is well-known that in one-phonon system with anharmonic cubic term, the frequency is a function of amplitude^{25,26}. The cubic term in two-phonon system should also cause the frequencies of both phonons to shift with ampli-

tudes, leading to “frequency renormalization”. Although there were reports about frequency renormalization of IR active mode^{24,27}, its influence on the dynamics of the two-phonon system, especially the rectification of Raman mode is yet to be uncovered. Here we tackle this problem by deriving an analytical expression of frequencies of IR and Raman modes (ω_{IR} and ω_R) as a function of their eigen amplitudes (a_R and a_{IR}), and analyzing its effect on Raman rectification in detail. As IR mode red-shifts under strong pump field, the linear increase of a_{IR} with pump field amplitude E_0 will be suppressed, leading to a saturation in the rectification amplitude of Raman active phonon. In Sec.II A the frequency-amplitude relation is derived, following the perturbation method suggested by Landau and Lifshitz²⁸. This method is analytically solvable, cheap and materials independent, compared with other realistic method, e.g. *ab initio* molecular dynamics¹⁹. In Sec.II B we discuss the a_{IR} - E_0 relation, numerical results of Raman rectification as a function of E_0 are given, along with some new features not revealed by analytical method. When the IR mode is degenerate, as shown in Sec.II C, the frequency of IR mode splits when resonantly pumped by elliptically or linearly polarized ultrashort mid-IR laser pulse, and Raman rectification and (oscillating) magnetization can be induced simultaneously. Finally, the frequency-amplitude relation can also be deduced from quantum perturbation method.

Nonlinear phononics makes use of tailored laser fields to resonantly drive the IR active phonons to large amplitudes²⁹. Our finding that the resonantly driven IR amplitude (and the induced rectification of Raman active phonon) tends to saturate under strong pump field indicates a dynamical constraint for accessible phonon displacement in quantum materials via nonlinear phononics. The amplitude saturation can be extended to system with strong spin-lattice interaction^{30,31}, and is more easily observed in systems with large coupling constant, e.g. the coupling between interlayer sliding phonon and intralayer shear phonon in WTe₂³². One way to improve the saturation amplitude is to use off-resonant laser field with slightly reduced frequency. The laser-induced dynamical multiferroicity^{18,33} is expected to occur in systems with phonon nonlinearity both in form $Q_R(Q_{IR,x}^2 - Q_{IR,y}^2)$ and $Q_R Q_{IR,x} Q_{IR,y}$, extending the candidate materials for future ultrafast data processing technology.

II. RESULTS AND DISCUSSION

A. The frequency-amplitude relation with $Q_R Q_{IR}^2$ coupling

Assume the IR active phonon is nondegenerate and has no associated phonon angular momentum^{34,35}. In the absence of damping, the Lagrangian of the two phonon system can be written as

$$L = \frac{1}{2} \sum_i \dot{Q}_i^2 - \frac{1}{2} \sum_i \omega_i^{(0)2} Q_i^2 + \frac{1}{2} g Q_R Q_{IR}^2 + Q_{IR} F(t) \quad (1)$$

where i runs over $\{R, IR\}$, the third term on the right denotes the coupling between Raman and IR modes, and the fourth term is the potential energy caused by laser pulse. To emphasize the renormalization of frequency, we use $\omega_i^{(0)}$ to denote the natural angular frequency, and ω_i to denote the observed angular frequency of the i mode. We assume $F(t) = Z_e^* E_0 e^{-t^2/\sigma^2} \cos(\gamma t)$, which corresponds to a pump pulse with Gaussian distribution. Here Z_e^* is Born effective charge of the IR mode, E_0 , σ and γ are the largest magnitude of the electric field, the time-domain duration, and the angular frequency of the laser pulse, respectively. Lagrangian's equation on Q_R and Q_{IR} then give

$$\ddot{Q}_R + \omega_R^{(0)2} Q_R = \frac{1}{2} g Q_{IR}^2 \quad (2a)$$

$$\ddot{Q}_{IR} + \omega_{IR}^{(0)2} Q_{IR} = g Q_R Q_{IR} + F(t) \quad (2b)$$

As a first step, we ignore $F(t)$ in Eq.(2b), namely we seek the solution at $t \rightarrow \infty$, *i.e.* the steady-state solution. Following Landau and Lifshitz²⁸, we obtain the following frequency-amplitude relations, which is valid to the second-order of coupling constant g ,

$$\omega_R = \omega_R^{(0)} - \frac{g^2 a_{IR}^2}{4 \omega_R^{(0)}} \frac{1}{(2 \omega_{IR}^{(0)})^2 - (\omega_R^{(0)})^2} \quad (3a)$$

$$\omega_{IR} = \omega_{IR}^{(0)} - \frac{g^2 a_{IR}^2}{8 \omega_{IR}^{(0)}} \left[\frac{1}{\omega_{IR}^{(0)2}} - \frac{1}{2} \frac{1}{(2 \omega_{IR}^{(0)})^2 - (\omega_R^{(0)})^2} \right] - \frac{g^2 a_R^2}{4 \omega_{IR}^{(0)}} \frac{1}{(2 \omega_{IR}^{(0)})^2 - (\omega_R^{(0)})^2} \quad (3b)$$

where $a_{IR/R}$ denote the zero-order oscillating amplitude of IR/Raman active mode. When condition $\sqrt{2} \omega_{IR}^{(0)} \gg \omega_R^{(0)}$ is satisfied, which is the usual case, the angular frequencies will decrease as the amplitudes increase. Eq.(3) allows us to infer the oscillation amplitudes a_{IR} and a_R from the frequencies ω_R and ω_{IR} if g is known, and is one of the main results of this work. We note that Fechner *et. al.*²⁷ had obtained a similar result (see Eq.(A1) and (A2) in the cited reference), which differs from ours in several places: (1) They considered a sinusoidal driving force, while a pulsed force is considered

here. (2) The second term on the right of their Eq.(A1) is proportional to a_R^2 , while ours is a_{IR}^2 , and their fourth term is proportional to a_{IR} , which should be a_{IR}^2 . (3) The third term on the right of their Eq.(A2) is proportional to $1/\omega_{IR}$, which should be $1/\omega_{IR}^2$ by dimension analysis. To second-order, the IR mode will oscillate in a superposition state with frequencies ω_{IR} , $\omega_{IR} \pm \omega_R$, $\omega_{IR} \pm 2\omega_R$ and $3\omega_{IR}$, while the Raman mode oscillates with frequencies ω_R , 0 , $2\omega_{IR}$ and $2\omega_{IR} \pm \omega_R$, where 0 is the rectified component, as shown schematically in Fig.1. The amplitudes of each component are listed in Table.I. The detailed deduction can be found in Appendix.A.

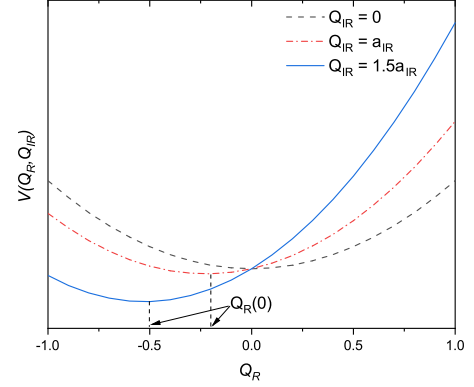


FIG. 1: The lattice potential of a two-phonon system with cubic term $Q_R Q_{IR}^2$. The rectification of Raman mode $Q_R(0)$ increases with the displacement of IR mode.

TABLE I: The angular frequencies and amplitudes of oscillation components for Q_R and Q_{IR} , to the second-order of coupling constant g . The expressions for ω_R and ω_{IR} are given by Eqs.(3).

Term	Angular frequency	Amplitude
$Q_R^{(0)}$	ω_R	a_R
$Q_R^{(1)}$	0	$\frac{1}{4} g a_{IR}^2$
	$2\omega_{IR}$	$\frac{\omega_R^{(0)2}}{\frac{1}{4} g a_{IR}^2}$
$Q_R^{(2)}$	$2\omega_{IR} - \omega_R$	$\frac{\frac{1}{4} g^2 a_R a_{IR}^2}{[\omega_{IR}^{(0)2} - (\omega_{IR}^{(0)} - \omega_R^{(0)})^2][\omega_R^{(0)2} - (2\omega_{IR}^{(0)} - \omega_R^{(0)})^2]}$
	$2\omega_{IR} + \omega_R$	$\frac{\frac{1}{4} g^2 a_R a_{IR}^2}{[\omega_{IR}^{(0)2} - (\omega_{IR}^{(0)} + \omega_R^{(0)})^2][\omega_R^{(0)2} - (2\omega_{IR}^{(0)} + \omega_R^{(0)})^2]}$
...
$Q_{IR}^{(0)}$	ω_{IR}	a_{IR}
$Q_{IR}^{(1)}$	$\omega_{IR} - \omega_R$	$\frac{\frac{1}{2} g a_R a_{IR}}{\omega_{IR}^{(0)2} - (\omega_{IR}^{(0)} - \omega_R^{(0)})^2}$
	$\omega_{IR} + \omega_R$	$\frac{\frac{1}{2} g a_R a_{IR}}{\omega_{IR}^{(0)2} - (\omega_{IR}^{(0)} + \omega_R^{(0)})^2}$
$Q_{IR}^{(2)}$	$\omega_{IR} - 2\omega_R$	$\frac{\frac{1}{4} g^2 a_R^2 a_{IR}}{[\omega_{IR}^{(0)2} - (\omega_{IR}^{(0)} - \omega_R^{(0)})^2][\omega_{IR}^{(0)2} - (\omega_{IR}^{(0)} - 2\omega_R^{(0)})^2]}$
	$\omega_{IR} + 2\omega_R$	$\frac{\frac{1}{4} g^2 a_R^2 a_{IR}}{[\omega_{IR}^{(0)2} - (\omega_{IR}^{(0)} + \omega_R^{(0)})^2][\omega_{IR}^{(0)2} - (\omega_{IR}^{(0)} + 2\omega_R^{(0)})^2]}$
	$3\omega_{IR}$	$\frac{\frac{1}{8} g^2 a_{IR}^2}{[\omega_R^{(0)2} - (2\omega_{IR}^{(0)})^2][\omega_{IR}^{(0)2} - (3\omega_{IR}^{(0)})^2]}$
...

B. The variation of amplitude of eigen IR mode with pump field

1. Linear increase of a_{IR} with E_0 under small field amplitude

In the previous section we've seen that the zero-order amplitudes a_R and a_{IR} determine all higher-order amplitudes, it is thus necessary to determine how a_R and a_{IR} vary with the amplitude of pump field E_0 . In other words, we wish to determine a_R and a_{IR} under different E_0 in Eq.(2). Suppose initially both a_R and a_{IR} equals to zero, and a_{IR} increases linearly with the pump field amplitude E_0 , the validity of which will be soon verified, then Q_{IR} is proportional to E_0 and Q_R is proportional to E_0^2 , leading to gQ_RQ_{IR} proportional to E_0^3 . As $F(t)$ is proportional to E_0 , under small pump field amplitude $F(t)$ is much larger than gQ_RQ_{IR} . The latter can safely be neglected and Eq.(2) becomes

$$\ddot{Q}_R + \omega_R^{(0)2} Q_R = \frac{1}{2} g Q_{IR}^2 \quad (4a)$$

$$\ddot{Q}_{IR} + \omega_{IR}^{(0)2} Q_{IR} = Z_e^* E_0 e^{-t^2/\sigma^2} \cos(\gamma t) \quad (4b)$$

It's then obvious that under small pump field, the IR mode will oscillate with frequency $\omega_{IR}^{(0)}$, while the Raman mode will be in first-order state $Q_R^{(1)}$, or oscillate around a displaced position with frequency $2\omega_{IR}^{(0)}$. In the following we show the oscillation amplitude a_{IR} of IR mode is proportional to E_0 .

When t is located in $[-\sigma, +\sigma]$, the external force is largest and the oscillating frequency of $Q_{IR}(t)$ is $\gamma/(2\pi)$ — the frequency of the laser pulse. As t increases, the force diminishes quickly, and Q_{IR} restores to oscillate with its normal frequency $\omega_{IR}^{(0)}$. The long-time oscillation amplitude can be obtained from energy conservation²⁸: The energy pumped in by the external force is half the squared modulus of Fourier component $\frac{1}{2}|F(\omega)|^2$ of the force at $\omega_{IR}^{(0)}$, where $F(\omega)$ is the Fourier transform of the force

$$\begin{aligned} F(\omega) &= \int_{-\infty}^{+\infty} Z_e^* E_0 e^{-t^2/\sigma^2} \cos(\gamma t) e^{-i\omega t} dt \\ &= \frac{\sqrt{\pi}}{2} Z_e^* E_0 \sigma [e^{-\frac{\sigma^2}{4}(\gamma-\omega)^2} + e^{-\frac{\sigma^2}{4}(\gamma+\omega)^2}] \end{aligned} \quad (5)$$

The energy pumped in should equal to the oscillation energy $\frac{1}{2}\omega_{IR}^{(0)2} a_{IR}^2$. For typical values of σ (~ 0.1 ps) and γ ($\sim 2\pi \times 10$ THz, same for ω), the second term ($\sim e^{-4\pi^2}$) in Eq.(5) can be neglected. Thus we have

$$a_{IR}(\gamma) = \frac{\sqrt{\pi} Z_e^* E_0 \sigma}{2\omega_{IR}^{(0)}} e^{-\frac{\sigma^2}{4}(\gamma-\omega_{IR}^{(0)})^2} \quad (6)$$

The linear relation between a_{IR} and E_0 is evident. In previous works^{20,21}, $\gamma = \omega_{IR}^{(0)}$ were assumed. Eq.(6) shows that the

oscillation amplitude is largest when $\gamma = \omega_{IR}^{(0)}$ and decreases as γ deviates from $\omega_{IR}^{(0)}$. The full width at half maximum (FWHM) of $F(\omega)$ is $4\sqrt{\ln 2}/\sigma$. Here the duration of the pulse σ should be chosen carefully: A small σ is required to obtain large amplitude in a wider frequency region, but at the same time it reduces the amplitude.

2. Saturation of a_{IR} with E_0 under large field amplitude

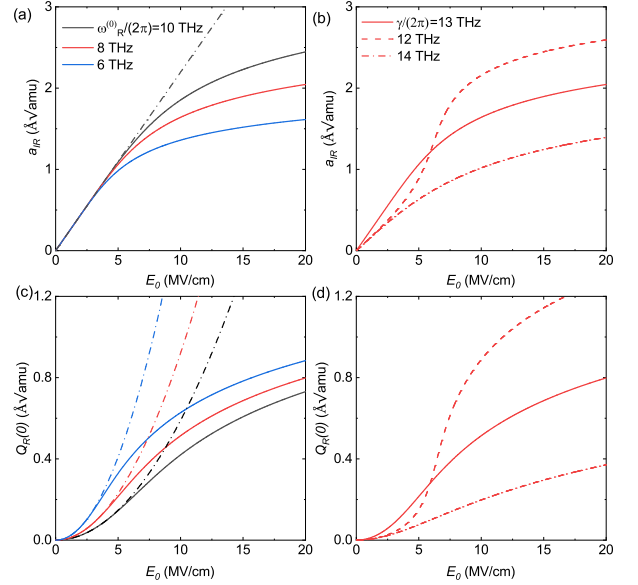


FIG. 2: The amplitudes of (a,b) eigen IR mode and (c,d) the corresponding rectified Raman mode as a function of pulse amplitude. $\omega_{IR}^{(0)}/(2\pi) = \gamma/(2\pi) = 13$ THz in (a) and (c), and $\omega_{IR}^{(0)}/(2\pi) = 8$ THz, $\omega_{IR}^{(0)}/(2\pi) = 13$ THz in (b) and (d). The dashed lines in (a) and (c) are linear and quadratic fitting curves, respectively.

As the pump field amplitude increases, the gQ_RQ_{IR} term increases more quickly than $F(t)$ and cannot be ignored. The inclusion of this term can be regarded as a renormalization of frequency³⁶ of the IR mode ($\omega_{IR}^{(0)} \rightarrow \sqrt{\omega_{IR}^{(0)2} - gQ_R}$), as long as the eigen Raman mode does not appear. Thus Eq.(4) can still be applied, but with $\omega_{IR}^{(0)}$ replaced by ω_{IR} , as given by Eq.(3b). For $\gamma = \omega_{IR}^{(0)}$, the frequency renormalization has the effect of decreasing the proportionality coefficient between a_{IR} and E_0 . By inserting Eq.(3b) (with $a_R = 0$) into Eq.(6) we get a transcendental equation about a_{IR}

$$a_{IR} \left(1 - \frac{c}{\omega_{IR}^{(0)}} a_{IR}^2\right) = \frac{\sqrt{\pi} Z_e^* E_0 \sigma}{2\omega_{IR}^{(0)}} e^{-\frac{\sigma^2}{4}(\gamma - \omega_{IR}^{(0)} + c a_{IR}^2)^2} \quad (7)$$

where Eq.(3b) is rewritten as $\omega_{IR} = \omega_{IR}^{(0)} - c a_{IR}^2$ and $c = \frac{g^2}{8\omega_{IR}^{(0)}} \left[\frac{1}{\omega_R^{(0)2}} - \frac{1}{(2\omega_{IR}^{(0)})^2 - (\omega_R^{(0)})^2} \right]$ is a constant for given $\omega_{IR}^{(0)}$,

$\omega_R^{(0)}$ and g . Eq.(7) can be solved numerically, and typical result is shown in Fig.2(a), where the trend of saturation of a_{IR} as E_0 increases is evident. Then by consulting Table.I, the rectification of Raman mode $Q_R(0)$ will deviate from quadratic behavior as E_0 increases, as shown in Fig.2(c). It is possible to realize larger rectification by using a pulse which is slightly off-resonant with the IR mode, at the cost of reducing a_{IR} at small E_0 , see Fig.2(b,d). This behavior was found in YTiO_3 ²³ previously, which can be extended to all two-phonon system with $Q_R Q_{IR}^2$ coupling and suitable $\omega_{IR}^{(0)}$, $\omega_R^{(0)}$.

3. The numerical results

To verify the above picture, we carry out numerical solutions of Eq.(2) with initial condition $(Q_R, \dot{Q}_R, Q_{IR}, \dot{Q}_{IR})|_{t_0} = (0, 0, 0, 0)$ by fourth-order Runge-Kutta method. Here t_0 is a negative time where $F(t)$ tends to zero. The parameters used are $\omega_{IR}^{(0)}/(2\pi) = 13$ THz, $\gamma = \omega_{IR}^{(0)}$, $\omega_R^{(0)}/(2\pi) = 8$ THz, $g = 0.2 \text{ eV}/(\sqrt{\text{amu}\text{\AA}})^3$ (a large g is used to illustrate the frequency shift, amu denotes the atomic mass unit), $\sigma = 0.21$ ps, $Z_e^* = 1.0 \text{ e}/\sqrt{\text{amu}}$ and E_0 varies from 0 to 35 MV/cm. The time step is $\Delta t = 0.625$ fs and $t_0 = -10 \times 2\pi/\omega_R^{(0)}$. Typical results are shown in Fig.3.

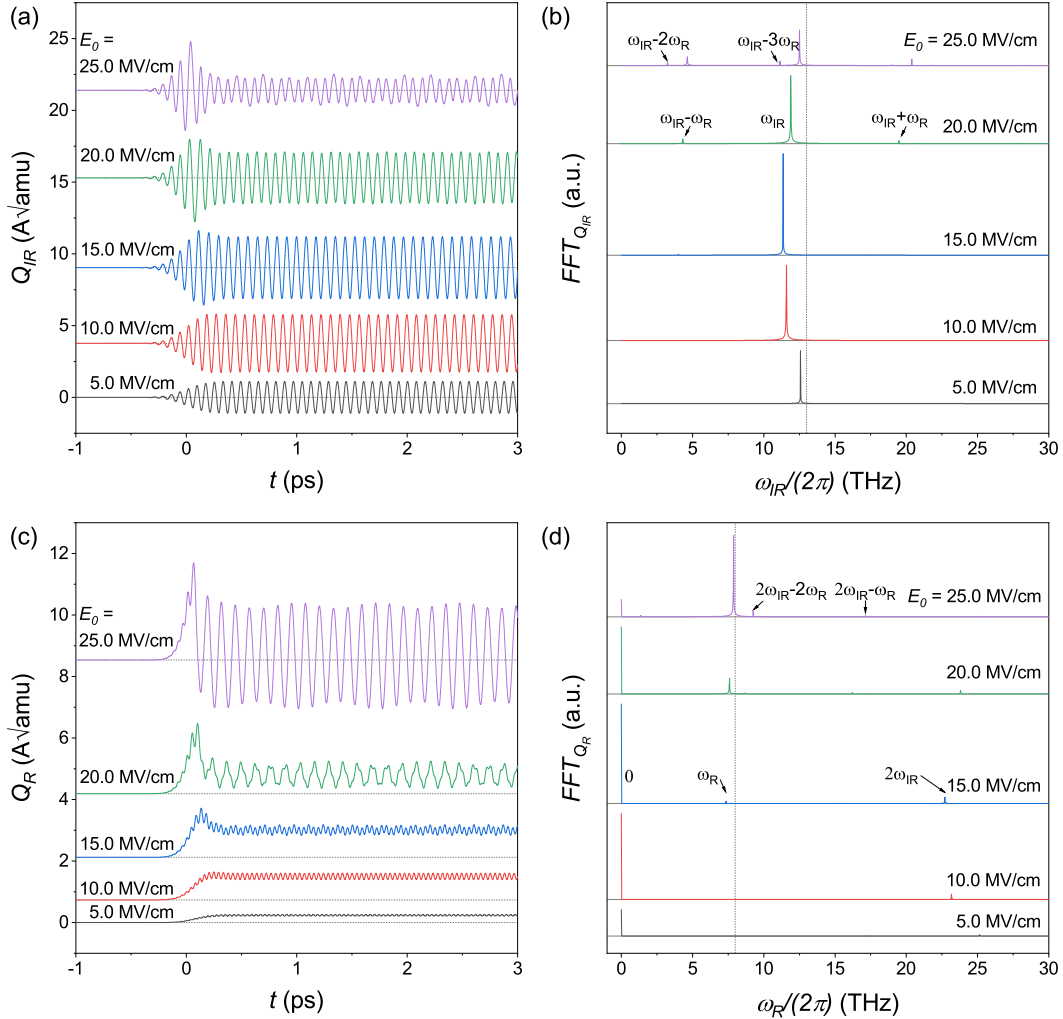


FIG. 3: The transient amplitudes of (a) IR and (c) Raman modes under pump pulses with different amplitudes, where damping effect is ignored. (b) and (d) are the amplitudes of the discrete Fourier transform of (a) and (c), respectively. The dashed lines in (b) and (d) indicate the natural frequencies of IR (13.0 THz) and Raman (8.0 THz) modes.

Under small amplitude of pump pulse (e.g. $E_0 = 5$ MV/cm), the IR mode oscillates in eigen mode with frequency ω_{IR} and

Raman mode oscillates in a superposition state of $2\omega_{IR}$ and 0, which is evident in the Fourier transform of the long-time

solution, as shown in Fig.3(b,d). This is consistent with the results in Sec.II A for $a_R = 0$, which indicates that only $Q_{IR}^{(0)}$ and $Q_R^{(1)}$ do not vanish. (The $3\omega_{IR}$ term in $Q_{IR}^{(2)}$ is also nonzero, but its magnitude is too small to be discerned.) As the pump pulse amplitude increases, the frequency of eigen IR mode red-shifts, which is clearly seen in Fig.3(b), and accordingly the $2\omega_{IR}$ -component of Raman mode also red-shifts, as shown in Fig.3(d).

The numerical results reveal two new phenomena: (1) As the amplitude of the pump pulse increases and becomes larger than a critical value (about 15 MV/cm here), the eigen Raman mode $Q_R^{(0)}$ with frequency ω_R will appear, as is evident in Fig.3(d), and afterwards nearly all the terms up to second-order (even third-order for IR phonon) appear. (2) The appearance of eigen Raman mode causes two possible results, The rectified Raman mode $Q_R(0)$ either reaches a maximum and then decreases with E_0 (e.g. for $\omega_R^{(0)}/(2\pi) = 8$ THz), or saturates in intermediate E_0 and continues to increase at larger E_0 (e.g. for $\omega_R^{(0)}/(2\pi) = 4$ THz), until the breakup of the system, as shown in Fig.4. Which one will happen seems to be determined by $\omega_R^{(0)}$ and $\omega_{IR}^{(0)}$, and the required pump field to realize saturation increases with $\omega_R^{(0)}$ for a given IR mode. Furthermore, when $\omega_R^{(0)} > \omega_{IR}^{(0)}$ and $\omega_{IR}^{(0)} \approx \frac{1}{2}\omega_R^{(0)}$, the rectification of Raman mode is weak, and another phenomena — the ionic Raman scattering occurs, as exemplified in Appendix.B.

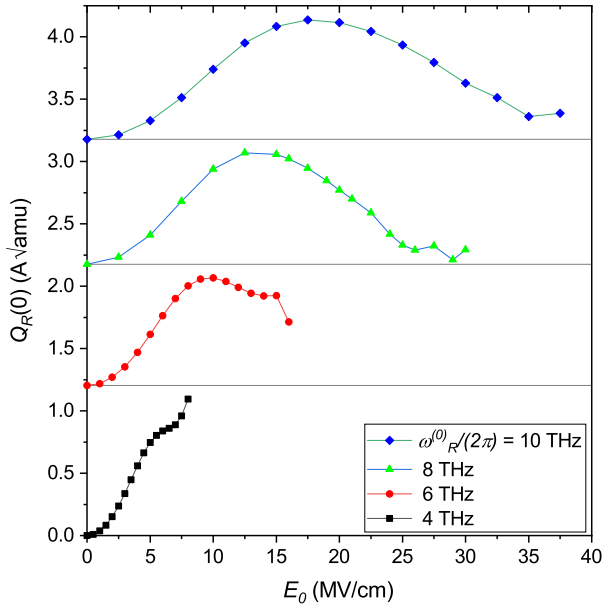


FIG. 4: (a) The variation of rectified Raman mode $Q_R(0)$ with E_0 for different frequencies of Raman mode, under resonant pumping. $\omega_{IR}^{(0)}/(2\pi) = 13$ THz.

C. Dynamically induced multiferroicity for degenerate IR mode

We proceed to show that if the IR mode is doubly degenerate and the coupling term is of form $Q_R(Q_{IR,x}^2 - Q_{IR,y}^2)$, e.g. B_1 and E modes in materials with point group D_{2d}^{20} , then it's possible to realize Raman rectification and magnetization transiently by resonantly exciting the IR mode with elliptically or linearly polarized mid-IR laser pulse, similar to the mechanism suggested by Paiva *et al.*¹⁸ recently. The pulse-induced multiferroicity discussed below assumes the following conditions to be satisfied: (1) The phonons have coupling of form $Q_R(Q_{IR,x}^2 - Q_{IR,y}^2)$. (2) Inversion symmetry is broken in the nonequilibrium state along the displaced Raman mode, and polarization is assumed to scale with the rectification amplitude of the Raman mode. (3) Meanwhile, the driven degenerate IR mode is expected to have large effective magnetic field³⁷, or large phonon magnetic moment³⁸ to make the oscillating magnetization observable. The equation of motion is

$$\ddot{Q}_R + \omega_R^{(0)2} Q_R = \frac{1}{2}g(Q_{IR,x}^2 - Q_{IR,y}^2) \quad (8a)$$

$$\ddot{Q}_{IR,x} + \omega_{IR}^{(0)2} Q_{IR,x} = gQ_R Q_{IR,x} + F_x(t) \quad (8b)$$

$$\ddot{Q}_{IR,y} + \omega_{IR}^{(0)2} Q_{IR,y} = -gQ_R Q_{IR,y} + F_y(t) \quad (8c)$$

For simplicity, we assume $F_x = eE_x(t)$ and $F_y = eE_y(t)$, where $E_x(t) = E_0 \cos(\phi) e^{-t^2/\sigma^2} \cos(\gamma t)$ and $E_y(t) = E_0 \sin(\phi) e^{-t^2/\sigma^2} \cos(\gamma t + \pi/2)$, with $\gamma = \omega_{IR}^{(0)}$. By the same method outlined in Appendix.A we obtain the frequencies and amplitudes of each mode, as summarized in Table.II in Appendix.C. The frequency-amplitude relation of the IR mode is

$$\omega_{IR,x} = \omega_{IR}^{(0)} - \frac{g^2(a_x^2 - a_y^2)}{8\omega_{IR}^{(0)}\omega_R^{(0)2}} + \frac{g^2 a_x^2}{16\omega_{IR}^{(0)}[(2\omega_{IR}^{(0)})^2 - (\omega_R^{(0)})^2]} - \frac{g^2 a_R^2}{4\omega_{IR}^{(0)}} \frac{1}{(2\omega_{IR}^{(0)})^2 - (\omega_R^{(0)})^2} \quad (9a)$$

$$\omega_{IR,y} = \omega_{IR}^{(0)} + \frac{g^2(a_x^2 - a_y^2)}{8\omega_{IR}^{(0)}\omega_R^{(0)2}} + \frac{g^2 a_y^2}{16\omega_{IR}^{(0)}[(2\omega_{IR}^{(0)})^2 - (\omega_R^{(0)})^2]} - \frac{g^2 a_R^2}{4\omega_{IR}^{(0)}} \frac{1}{(2\omega_{IR}^{(0)})^2 - (\omega_R^{(0)})^2} \quad (9b)$$

where the first terms on the right have opposite signs. The second term is usually much smaller than the first term for $\omega_{IR}^{(0)} > \omega_R^{(0)}$, and the third term does not occur at small pump field ($a_R = 0$). In the circumstance $a_x \neq a_y$, the original degenerate IR mode will become nondegenerate.

For linearly polarized mid-IR pulse along x ($\phi = 0$) or y ($\phi = \pi/2$) direction, only $Q_{IR,x}$ or $Q_{IR,y}$ will be nonzero, and Eq.(8) returns to Eq.(2). The rectification of Raman mode will be switched between x and y polarized light, while the IR mode has no phonon angular momentum, see Fig.5(a1,b1,c1).

When pumped by elliptically polarized mid-IR pulse ($0 < \phi < \pi/4$), $Q_{IR,x}$ and $Q_{IR,y}$ are both excited, but to different amplitudes ($a_x > a_y$), the Raman mode will be oscillating in $2\omega_{IR,x}$ and $2\omega_{IR,y}$ around a rectified position $\langle Q_R \rangle = g(a_x^2 - a_y^2)/(4\omega_R^{(0)2})$, while the frequency of degenerate IR mode will be split into $\sqrt{\omega_{IR}^{(0)2} \mp g\langle Q_R \rangle}$, which is similar to Eq.(9) in that the last two terms are neglected. This frequency splitting then leads to nonzero phonon angular momentum $L_{IR,z}$ and magnetization $M_z = \mu_{ph}L_{IR,z}/(\hbar V_c)$, which oscillate in superposition state of frequencies $(\omega_{IR,y} \mp \omega_{IR,x})/2$ with amplitudes $a_x a_y (\omega_{IR,y} \pm \omega_{IR,x})/2$, as shown in Fig.5(a2,b2,c2). Here μ_{ph} is the phonon magnetic moment, \hbar is the reduced Planck constant, and V_c is the unit cell volume. If the Raman rectification

leads to ferroelectric phase and the phonon magnetic moment is of order μ_B , the dynamical multiferroicity will occur.

Furthermore, it is also possible to induce Raman rectification and oscillating magnetization simultaneously by linearly polarized mid-IR pulse not along x , y or $x \pm y$ direction, as shown in Fig.5(a4,b4,c4). The sign of Raman rectification can be switched by changing the long axis of elliptically polarized pulse to along y , or the angle of linearly polarized pulse, while the direction of angular momentum in the first half-cycle can be switched by changing the handedness of elliptically polarized pulse, or using the x/y -symmetric partner of linearly polarized pulse.

For circularly polarized pulse ($\phi = \pi/4$), $Q_{IR,x}$ and $Q_{IR,y}$ are excited to the same amplitudes ($a_x = a_y$), and the rectification of Raman mode disappears (see Table.II). The frequency of IR mode does not split, but increases slightly as the strength of pump pulse increases. The IR mode has angular momentum with amplitude $a_x^2 \omega_{IR,x}$.

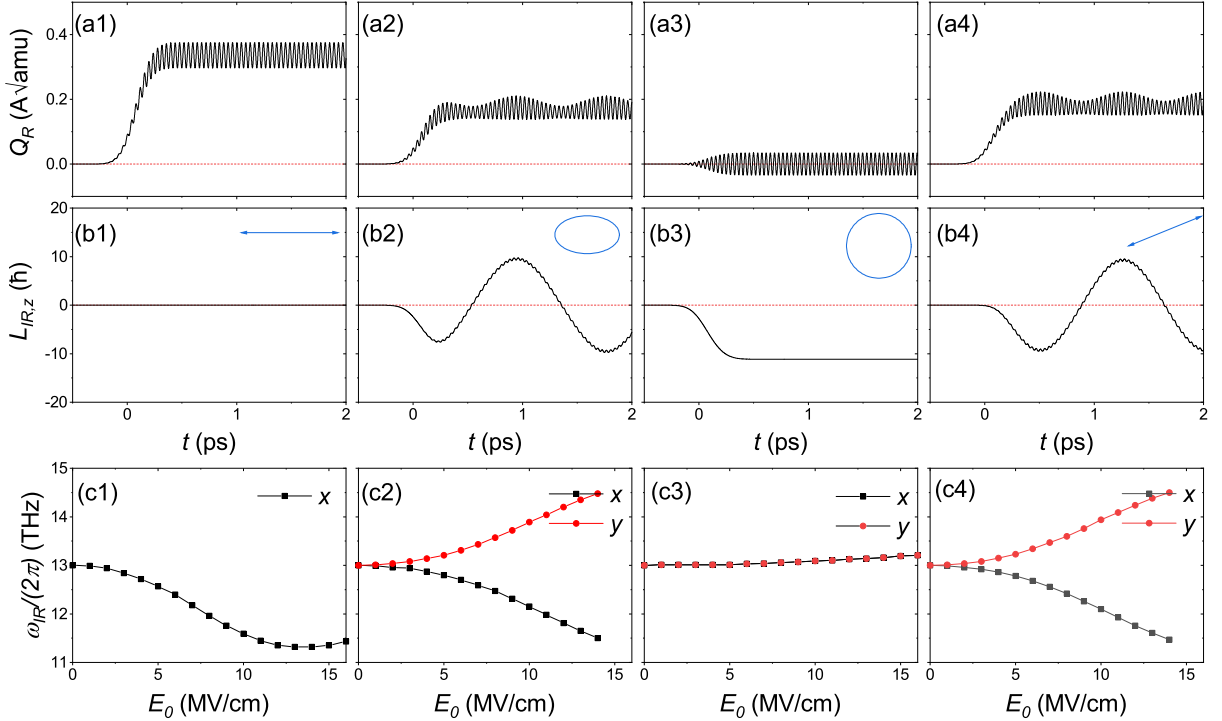


FIG. 5: The transient amplitudes of (a) Raman mode and (b) angular momentum of IR modes under pump pulses with amplitude $E_0 = 6$ MV/cm and (1) linear polarization along x , (2) elliptical polarization with $\phi = \pi/6$, (3) circular polarization and (4) linear polarization $\pi/6$ with respect to x . (c) The frequency of IR mode as function of pump pulse amplitude.

D. Discussion

We note that the saturation of Raman rectification are more easily observed in systems with larger coupling constant. This can be seen as follows, suppose Q_{IR} and Q_R are solutions of

Eq.(2) at coupling constant g and pump field E_0 , if $g \rightarrow kg$, where k is a constant, then $Q_{IR} \rightarrow \frac{1}{k}Q_{IR}$, $Q_R \rightarrow \frac{1}{k}Q_R$ and $E_0 \rightarrow \frac{1}{k}E_0$ will also be a solution for the new coupling constant. This means that both the saturation amplitude (if it exists for the two-phonon system) and the required pump field to realize

saturation will be reduced.

The frequency renormalization of IR mode can still be observed if damping effect is included. The corresponding Fourier transform of Q_{IR} will be asymmetrically peaked at ω_{IR} and broadens as E_0 increases. The rectification behavior of Raman mode is somehow difficult to be discerned — the peak of Q_R near $t = 0$ increases as E_0 increases, but the peak of Fourier transform of Q_R at 0 tends to saturate and broadens at large E_0 . It should be pointed out that the peak of Q_R near $t = 0$ is not the rectified Raman mode we've discussed above. As can be seen in Fig.3(c), the Raman mode also has a peak near $t = 0$ at large E_0 , but that's not the rectified Raman mode, which is the rectified component of long-time solution $Q_R(t)$, where $E(t)$ approaches zero.

Finally, the discussion on “dynamically induced multiferroicity” can be applied to systems with coupling of form $Q'_{IR,x}Q'_{IR,y}Q_R$, simply by coordinate transformation $Q_{IR,x} = (Q'_{IR,x} + Q'_{IR,y})/\sqrt{2}$ and $Q_{IR,y} = (Q'_{IR,x} - Q'_{IR,y})/\sqrt{2}$. The “overshoot of magnetization upon decay” in Paiva *et. al.*'s work¹⁸ reveals the hidden oscillating behavior of magnetization discussed above, covered up by damping effect.

III. CONCLUSION

In conclusion, we have given an analytical solution of the two-phonon system coupled by $gQ_RQ_{IR}^2$ to second order of coupling constant g . The frequency renormalization of IR mode suppresses the linear increase of a_{IR} with driving amplitude E_0 , eventually leading to a saturation of the rectified amplitude of the Raman phonon. This finding suggests that under the mechanism of anharmonic coupling, it might not be possible to drive a crystalline system to any displacement along the eigenvector of Raman phonon before the breaking of the system, even though it is allowed by the potential energy landscape. For degenerate IR mode, the frequency splitting leads to simultaneous Raman rectification and oscillating magnetization, when pumped by elliptically or linearly polarized pulse. The saturation phenomena can be tested on systems with large anharmonic coupling constant by femtosecond x-ray measurement. Our work extends the dynamical multiferroicity from systems with coupling $Q_{IR,x}Q_{IR,y}Q_R$ to systems with coupling $Q_R(Q_{IR,x}^2 - Q_{IR,y}^2)$, and the method can be readily applied to other anharmonic terms, *e.g.* $Q_R^2Q_{IR}^2$.

ACKNOWLEDGMENTS

Y.Z. would like to thank H. Mao for discussions about Fast Fourier transformation and the National Supercomputer Center in Guangzhou for computational supports. This work is supported by Zhejiang Provincial Natural Science Foundation (Grant No. LQ21A040010).

Appendix A: Deduction of frequency-amplitude relations

Suppose the solution of Eq. (2) can be written as a series of successive approximations:

$$Q_R = Q_R^{(0)} + Q_R^{(1)} + Q_R^{(2)} + \dots \quad (\text{A1a})$$

$$Q_{IR} = Q_{IR}^{(0)} + Q_{IR}^{(1)} + Q_{IR}^{(2)} + \dots \quad (\text{A1b})$$

where $Q_R^{(0)} = a_{RCOS}(\omega_R t)$ and $Q_{IR}^{(0)} = a_{IRCOS}(\omega_{IR} t)$. The difference in initial phases between $Q_R^{(0)}$ and $Q_{IR}^{(0)}$ does not influence the following results and is taken to be zero. The superscript (i) denotes that this term is proportional to the i -th power of the coupling constant g . The frequencies ω_R and ω_{IR} are exact and can be expanded similarly as

$$\omega_R = \omega_R^{(0)} + \omega_R^{(1)} + \omega_R^{(2)} + \dots \quad (\text{A2a})$$

$$\omega_{IR} = \omega_{IR}^{(0)} + \omega_{IR}^{(1)} + \omega_{IR}^{(2)} + \dots \quad (\text{A2b})$$

Substitute Eq.(A1) and Eq.(A2) into Eq.(2) and equate the coefficients of identical powers of g , recursively solvable equations will be obtained. Retaining terms of the first-order, we obtain for $Q_R^{(1)}$ and $Q_{IR}^{(1)}$ the equations

$$\ddot{Q}_R^{(1)} + \omega_R^{(0)2} Q_R^{(1)} = \frac{1}{2} g a_{IR}^2 \cos^2(\omega_{IR} t) + 2 \omega_R^{(0)} \omega_R^{(1)} a_{RCOS}(\omega_R t) \quad (\text{A3a})$$

$$\ddot{Q}_{IR}^{(1)} + \omega_{IR}^{(0)2} Q_{IR}^{(1)} = g a_R a_{IRCOS}(\omega_R t) \cos(\omega_{IR} t) + 2 \omega_{IR}^{(0)} \omega_{IR}^{(1)} a_{IRCOS}(\omega_{IR} t) \quad (\text{A3b})$$

By requiring the resonant terms ($\cos(\omega_R t)$ and $\cos(\omega_{IR} t)$) should vanish in Eq.(A3), we have $\omega_R^{(1)} = \omega_{IR}^{(1)} = 0$, and

$$Q_R^{(1)} = \frac{\frac{1}{4} g a_{IR}^2}{\omega_R^{(0)2}} + \frac{\frac{1}{4} g a_{IR}^2}{\omega_R^{(0)2} - (2\omega_{IR}^{(0)})^2} \cos(2\omega_{IR} t) \quad (\text{A4a})$$

$$Q_{IR}^{(1)} = \frac{1}{2} g a_R a_{IR} \left[\frac{\cos(\omega_{IR} - \omega_R) t}{\omega_{IR}^{(0)2} - (\omega_{IR}^{(0)} - \omega_R^{(0)})^2} + \frac{\cos(\omega_{IR} + \omega_R) t}{\omega_{IR}^{(0)2} - (\omega_{IR}^{(0)} + \omega_R^{(0)})^2} \right] \quad (\text{A4b})$$

It is obvious from Eq.(A4a) that Q_R will oscillate in $2\omega_{IR}$ around a displaced position, or Q_R is rectified, even if Q_R is initially at rest ($(Q_R, \dot{Q}_R) = (0, 0)$). To obtain better rectification, the amplitude of displacement should be much larger than those of oscillations, *i.e.* $\sqrt{2}\omega_{IR}^{(0)} \gg \omega_R^{(0)}$ and $\frac{1}{4} g a_{IR}^2 \gg a_R$. Eq.(A4b) indicates that additional oscillations with frequencies $\omega_{IR} \pm \omega_R$ are superposed on eigen mode of Q_{IR} ³⁹.

In a similar manner, by retaining terms of the second-order, we obtain equations for $Q_R^{(2)}$ and $Q_{IR}^{(2)}$,

$$\ddot{Q}_R^{(2)} + \omega_R^{(0)2} Q_R^{(2)} = g a_{IRCOS}(\omega_{IR} t) Q_{IR}^{(1)} + 2 \omega_R^{(0)} \omega_R^{(2)} a_{RCOS}(\omega_R t) \quad (\text{A5a})$$

$$\begin{aligned} \ddot{Q}_{IR}^{(2)} + \omega_{IR}^{(0)2} Q_{IR}^{(2)} &= g(a_R \cos(\omega_R t) Q_{IR}^{(1)} + a_{IR} \cos(\omega_R t) Q_R^{(1)}) \\ &\quad + 2\omega_{IR}^{(0)} \omega_{IR}^{(2)} a_{IR} \cos(\omega_{IR} t) \end{aligned} \quad (\text{A5b})$$

Substitute Eq.(A4) into the right side of Eq.(A5) and let the resonant terms vanish, we then obtain the shift of frequencies as a function of the amplitudes as shown in the main text, Eq.(3). The remaining terms on the right side of Eq.(A5) then give

$$\begin{aligned} Q_R^{(2)} &= \frac{1}{4} g^2 a_R a_{IR}^2 \left\{ \frac{\cos[(2\omega_{IR} - \omega_R)t]}{[\omega_{IR}^{(0)2} - (\omega_{IR}^{(0)} - \omega_R^{(0)})^2][\omega_R^{(0)2} - (2\omega_{IR}^{(0)} - \omega_R^{(0)})^2]} \right. \\ &\quad \left. + \frac{\cos[(2\omega_{IR} + \omega_R)t]}{[\omega_{IR}^{(0)2} - (\omega_{IR}^{(0)} + \omega_R^{(0)})^2][\omega_R^{(0)2} - (2\omega_{IR}^{(0)} + \omega_R^{(0)})^2]} \right\} \end{aligned} \quad (\text{A6})$$

and

$$\begin{aligned} Q_{IR}^{(2)} &= \frac{1}{4} g^2 a_R^2 a_{IR} \left\{ \frac{\cos[(\omega_{IR} - 2\omega_R)t]}{[\omega_{IR}^{(0)2} - (\omega_{IR}^{(0)} - \omega_R^{(0)})^2][\omega_{IR}^{(0)2} - (\omega_{IR}^{(0)} - 2\omega_R^{(0)})^2]} \right. \\ &\quad \left. + \frac{\cos[(\omega_{IR} + 2\omega_R)t]}{[\omega_{IR}^{(0)2} - (\omega_{IR}^{(0)} + \omega_R^{(0)})^2][\omega_{IR}^{(0)2} - (\omega_{IR}^{(0)} + 2\omega_R^{(0)})^2]} \right\} \\ &\quad + \frac{1}{8} g^2 a_{IR}^3 \frac{\cos(3\omega_{IR}t)}{[\omega_R^{(0)2} - (2\omega_{IR}^{(0)})^2][\omega_{IR}^{(0)2} - (3\omega_{IR}^{(0)})^2]} \end{aligned} \quad (\text{A7})$$

Eqs.(A6) and (A7) show that up to second order of smallness, additional components with frequencies $2\omega_{IR} \pm \omega_R$ are added on Q_R , and components with frequencies $\omega_{IR} \pm 2\omega_R$ and $3\omega_{IR}$ are superposed on Q_{IR} .

The above processes can be extended to higher orders and more modes will occur. For example, $\omega_R^{(3)} = \omega_{IR}^{(3)} = 0$, $Q_R^{(3)}$ contains additional oscillations of frequencies $2\omega_{IR} \pm 2\omega_R$, $2\omega_R$, and $4\omega_{IR}$, and $Q_{IR}^{(3)}$ contains additional frequencies $\omega_{IR} \pm 3\omega_R$ and $3\omega_{IR} \pm \omega_R$. However, their amplitudes are much weaker and will not be considered here.

Appendix B: The case of ionic Raman scattering

Consider the special case when $\omega_{IR}^{(0)} \approx \frac{1}{2}\omega_R^{(0)}$, which we show corresponds to the ‘‘sum-frequency ionic Raman scattering’’⁴⁰. By referring to Table.I it’s clear that $Q_R^{(1)}(2\omega_{IR})$ has large amplitude due to the denominator $\omega_R^{(0)2} - (2\omega_{IR}^{(0)})^2$ approaches zero. Meanwhile, the $Q_R^{(0)}(\omega_R)$ mode will also be excited, with a_R of the same magnitude with $\frac{1}{4}ga_{IR}^2/(\omega_R^{(0)2} - (2\omega_{IR}^{(0)})^2)$. As a result, Q_R will oscillate in slightly different frequencies (ω_R and $2\omega_{IR}$) and form beats, with beat frequency $\omega_R - 2\omega_{IR}$, see Fig.6 for the coupled A_1 modes (15.3 THz for Raman and 7.4 THz for IR phonons) of BiFeO_3 ⁴⁰. Lastly, the rectification of Raman mode can be neglected since the rectification amplitude $\frac{1}{4}ga_{IR}^2/\omega_R^{(0)2}$ is much smaller than that of $2\omega_{IR}$ mode $\frac{1}{4}ga_{IR}^2/(\omega_R^{(0)2} - (2\omega_{IR}^{(0)})^2)$.

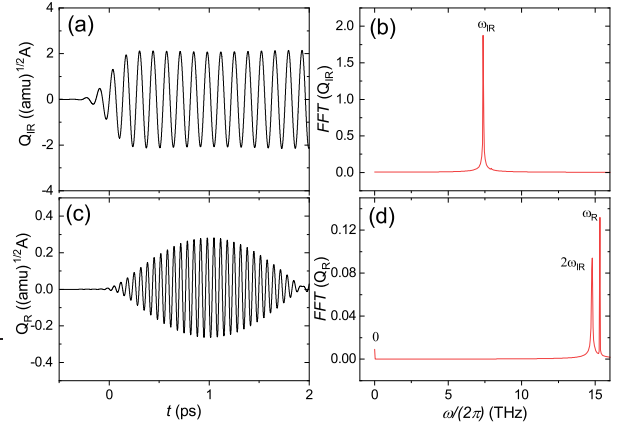


FIG. 6: (a) $Q_{IR}(t)$ and (c) $Q_R(t)$ under pump pulse with $E_0 = 8$ MV/cm, $\omega_{IR}^{(0)}/(2\pi) = 7.4$ THz, $\omega_R^{(0)}/(2\pi) = 15.3$ THz, other parameters are the same with Juraschek *et. al.*’s work on BiFeO_3 ⁴⁰. (b) and (d) are the amplitudes of Fourier transform of long-time solutions of Q_{IR} and Q_R , respectively.

Appendix C: The case of degenerate IR mode

TABLE II: The angular frequencies and amplitudes of components for Q_R , $Q_{IR,x}$ and $Q_{IR,y}$ to the first-order. The expressions for $\omega_{IR,x}$ and $\omega_{IR,y}$ are given by Eqs.(9).

Term	Angular frequency	Amplitude
$Q_R^{(0)}$	ω_R	a_R
$Q_R^{(1)}$	0	$\frac{1}{4}g(a_x^2 - a_y^2)$
	$2\omega_{IR,x}$	$\frac{\omega_R^{(0)2}}{\frac{1}{4}ga_x^2}$
	$2\omega_{IR,y}$	$\frac{\omega_R^{(0)2} - (2\omega_{IR}^{(0)})^2}{\frac{1}{4}ga_y^2}$
...
$Q_{IR,x}^{(0)}$	$\omega_{IR,x}$	a_x
$Q_{IR,x}^{(1)}$	$\omega_{IR,x} - \omega_R$	$\frac{\frac{1}{2}ga_R a_x}{\omega_{IR}^{(0)2} - (\omega_{IR}^{(0)} - \omega_R^{(0)})^2}$
	$\omega_{IR,x} + \omega_R$	$\frac{\frac{1}{2}ga_R a_x}{\omega_{IR}^{(0)2} - (\omega_{IR}^{(0)} + \omega_R^{(0)})^2}$
...
$Q_{IR,y}^{(0)}$	$\omega_{IR,y}$	a_y
$Q_{IR,y}^{(1)}$	$\omega_{IR,y} - \omega_R$	$\frac{\frac{1}{2}ga_R a_y}{\omega_{IR}^{(0)2} - (\omega_{IR}^{(0)} - \omega_R^{(0)})^2}$
	$\omega_{IR,y} + \omega_R$	$\frac{\frac{1}{2}ga_R a_y}{\omega_{IR}^{(0)2} - (\omega_{IR}^{(0)} + \omega_R^{(0)})^2}$
...

Appendix D: The quantum mechanical treatment

In this section we show that the frequency renormalization can be obtained by perturbation method to the second order. The Hamiltonian of the coupled two-phonon system is

$$\hat{H} = \hat{H}_0 + \hat{H}_1 \quad (\text{D1})$$

where $\hat{H}_0 = \frac{1}{2}\hat{p}_R^2 + \frac{1}{2}\omega_R^{(0)2}\hat{Q}_R^2 + \frac{1}{2}\hat{p}_{IR}^2 + \frac{1}{2}\omega_{IR}^{(0)2}\hat{Q}_{IR}^2$ and $\hat{H}_1 = -\frac{1}{2}g\hat{Q}_R\hat{Q}_{IR}$. Here \hat{Q} has the dimension of $\text{mass}^{1/2} \times \text{length}$, and \hat{H}_0 corresponds to a two-dimensional harmonic oscillator with eigenvalues $E_{n,m}^{(0)} = (n + \frac{1}{2})\hbar\omega_R^{(0)} + (m + \frac{1}{2})\hbar\omega_{IR}^{(0)}$, $n, m = 0, 1, 2, \dots$. The eigenfunctions are $\psi_{n,m}(Q_R, Q_{IR}) = u_n(Q_R)u_m(Q_{IR})$, with

$$u_n(Q_i) = N_n H_n(\alpha_i Q_i) e^{-\frac{1}{2}\alpha_i^2 Q_i^2} \quad (\text{D2})$$

where $N_n = (\frac{\alpha_i}{\sqrt{\pi 2^n n!}})^{1/2}$ is the normalization constant, $\alpha_i = (\omega_i^{(0)}/\hbar)^{1/2}$, $i = R, IR$ and H_n is the n th Hermite polynomial.

The eigenvalues of \hat{H} up to second-order are

$$E_{n,m} = E_{n,m}^{(0)} + \langle n, m | \hat{H}_1 | n, m \rangle + \sum_{n', m' \neq n, m} \frac{|\langle n, m | \hat{H}_1 | n', m' \rangle|^2}{E_{n,m}^{(0)} - E_{n', m'}^{(0)}} \quad (\text{D3})$$

By virtue of

$$\langle n | \hat{Q}_i | m \rangle = \begin{cases} \frac{1}{\alpha_i} \sqrt{\frac{n}{2}}, & m = n - 1 \\ \frac{1}{\alpha_i} \sqrt{\frac{n+1}{2}}, & m = n + 1 \\ 0, & \text{otherwise} \end{cases} \quad (\text{D4})$$

and

$$\langle n | \hat{Q}_i^2 | m \rangle = \begin{cases} \frac{1}{2\alpha_i^2} \sqrt{(n-1)n}, & m = n - 2 \\ \frac{1}{2\alpha_i^2} \sqrt{2n+1}, & m = n \\ \frac{1}{2\alpha_i^2} \sqrt{(n+1)(n+2)}, & m = n + 2 \\ 0, & \text{otherwise} \end{cases} \quad (\text{D5})$$

the first-order term in Eq.(D3) vanishes. There are only six second-order terms, corresponding to $n' = n \pm 1$ and $m' = m, m \pm 2$. A little algebraic efforts lead to

$$E_{n,m} = \hbar\omega_R(n + \frac{1}{2}) + \hbar\omega_{IR}(m + \frac{1}{2}) + \Delta E_0 \quad (\text{D6})$$

where

$$\omega_R = \omega_R^{(0)} - \frac{g^2 \langle m | Q_{IR}^2 | m \rangle}{4\omega_R^{(0)}} \frac{1}{(2\omega_{IR}^{(0)})^2 - (\omega_R^{(0)})^2} \quad (\text{D7a})$$

$$\omega_{IR} = \omega_{IR}^{(0)} - \frac{g^2 \langle m | Q_{IR}^2 | m \rangle}{8\omega_{IR}^{(0)}} \left[\frac{1}{\omega_R^{(0)2}} - \frac{1}{2} \frac{1}{(2\omega_{IR}^{(0)})^2 - \omega_R^{(0)2}} \right] - \frac{g^2 \langle n | Q_R^2 | n \rangle}{4\omega_{IR}^{(0)}} \frac{1}{(2\omega_{IR}^{(0)})^2 - (\omega_R^{(0)})^2} \quad (\text{D7b})$$

$$\Delta E_0 = \frac{3}{64} \frac{g^2 \hbar^2}{\omega_{IR}^{(0)2}} \frac{1}{(2\omega_{IR}^{(0)})^2 - (\omega_R^{(0)})^2} \quad (\text{D7c})$$

It's clear that the frequency renormalization has the same form with Eq.(3), if a_{IR} is replaced by $|\langle m | Q_{IR}^2 | m \rangle|^{1/2}$ and a_R by $|\langle n | Q_R^2 | n \rangle|^{1/2}$. Different from the classical treatment, the initial values of Q_R and Q_{IR} can not be assumed zero due to

the zero-point energy, and can be estimated by requiring that $\frac{1}{2}\omega_i^{(0)2}Q_i^2 = \frac{1}{2}\hbar\omega_i^{(0)}$, which then gives $Q_i|_{t_0} = \sqrt{\hbar/\omega_i^{(0)}}$, $i = R, IR$.

* zengyj@hdu.edu.cn

¹ B. Liu, H. Bromberger, A. Cartella, T. Gebert, M. Forst, and A. Cavalleri, *Opt Lett* **42**, 129 (2017).

² C. Vicario, A. Trisorio, S. Allenspach, C. Rüegg, and F. Giorgianni, *Applied Physics Letters* **117**, 101101 (2020).

³ D. Pavicevic, M. Nishida, J. Song, M. Buzzi, and A. Cavalleri, "Tunable narrowband thz generation in the organic crystal bna,"

(2025), arXiv:2510.22284.

⁴ D. M. Juraschek, M. Fechner, and N. A. Spaldin, *Phys Rev Lett* **118**, 054101 (2017).

⁵ F. Libbi, A. Johansson, L. Monacelli, and B. Kozinsky, *NPJ Comput Mater* **11**, 102 (2025).

⁶ A. Levchuk, R. Busselez, G. Vaudel, P. Ruello, V. Juvé, and B. Arnaud, "Nonlinear phononics in bi2te3 nanoscale thin films:"

- A theoretical approach,” (2025), arXiv:2501.04101.
- 7 B. I. Eraso-Solarte and Y. Ren, “Dissipative nonlinear phononics: Nonequilibrium quasiperiodic order in light-driven spin-phonon system,” (2026), arXiv:2603.13513.
 - 8 A. Subedi, *Physical Review B* **92**, 214303 (2015).
 - 9 A. Subedi, *Physical Review B* **95**, 134113 (2017).
 - 10 P. Chen, C. Paillard, H. J. Zhao, J. Iniguez, and L. Bellaiche, *Nat Commun* **13**, 2566 (2022).
 - 11 A. S. Disa, T. F. Nova, and A. Cavalleri, *Nature Physics* **17**, 1087 (2021).
 - 12 R. Mankowsky, A. Subedi, M. Forst, S. O. Mariager, M. Chollet, H. T. Lemke, J. S. Robinson, J. M. Glowia, M. P. Minitti, A. Frano, M. Fechner, N. A. Spaldin, T. Loew, B. Keimer, A. Georges, and A. Cavalleri, *Nature* **516**, 71 (2014).
 - 13 A. S. Disa, M. Fechner, T. F. Nova, B. Liu, M. Först, D. Prabhakaran, P. G. Radaelli, and A. Cavalleri, *Nature Physics* **16**, 937 (2020).
 - 14 R. Mankowsky, A. von Hoegen, M. Forst, and A. Cavalleri, *Phys Rev Lett* **118**, 197601 (2017).
 - 15 M. Fechner, M. Forst, G. Orenstein, V. Krapivin, A. S. Disa, M. Buzzi, A. von Hoegen, G. de la Pena, Q. L. Nguyen, R. Mankowsky, M. Sander, H. Lemke, Y. Deng, M. Trigo, and A. Cavalleri, *Nat Mater* **23**, 363 (2024).
 - 16 C. P. Romao and D. M. Juraschek, *ACS Nano* **18**, 29550 (2024).
 - 17 Z. Zeng, M. Först, M. Fechner, M. Buzzi, E. B. Amuah, C. Putzke, P. J. W. Moll, D. Prabhakaran, P. G. Radaelli, and A. Cavalleri, *Science* **387**, 431 (2025).
 - 18 C. Paiva, M. Fechner, and D. M. Juraschek, *Phys. Rev. Lett.* **135**, 066702 (2025).
 - 19 D. Shin, A. Rubio, and P. Tang, *Phys. Rev. Lett.* **132**, 016603 (2024).
 - 20 P. G. Radaelli, *Physical Review B* **97**, 085145 (2018).
 - 21 A. Subedi, A. Cavalleri, and A. Georges, *Physical Review B* **89**, 220301 (2014).
 - 22 M. Först, C. Manzoni, S. Kaiser, Y. Tomioka, Y. Tokura, R. Merlin, and A. Cavalleri, *Nature Physics* **7**, 854 (2011).
 - 23 M. Gu and J. M. Rondinelli, *Phys. Rev. B* **98**, 024102 (2018).
 - 24 M. Fechner and N. A. Spaldin, *Phys. Rev. B* **94**, 134307 (2016).
 - 25 M. Hase, M. Kitajima, S.-i. Nakashima, and K. Mizoguchi, *Phys. Rev. Lett.* **88**, 067401 (2002).
 - 26 K. Sokolowski-Tinten, C. Blome, J. Blums, A. Cavalleri, C. Dietrich, A. Tarasevitch, I. Uschmann, E. Förster, M. Kammler, M. Horn-von Hoegen, and D. von der Linde, *Nature* **422**, 287 (2003).
 - 27 M. Fechner, A. Sukhov, L. Chotorlishvili, C. Kenel, J. Berakdar, and N. A. Spaldin, *Phys. Rev. Mater.* **2**, 064401 (2018).
 - 28 L. D. Landau and E. M. Lifshitz, *Mechanics Third Edition, chapter 5* (Elsevier Butterworth-Heinemann, 1976).
 - 29 M. Henstridge, M. Först, E. Rowe, M. Fechner, and A. Cavalleri, *Nature Physics* **18**, 457 (2022).
 - 30 B. Ilyas, T. Luo, A. von Hoegen, E. Viñas Boström, Z. Zhang, J. Park, J. Kim, J.-G. Park, K. A. Nelson, A. Rubio, and N. Gedik, *Nature* **636**, 609 (2024).
 - 31 T. Lu, A. Wu, J. Li, M. Zeng, D. Cheng, C. Liu, J. Gong, and X. Li, “Ultrafast cooperative electronic, structural, and magnetic switching in an altermagnet,” (2025), arXiv:2509.11722.
 - 32 J. G. Horstmann, C. Emeis, A. Caviezel, Q. N. Meier, N. Wyler, T. Lottermoser, F. Caruso, and M. Fiebig, “Coherent phonon control beyond amplitude saturation in a sliding ferroelectric,” (2025), arXiv:2508.16422.
 - 33 M. Pols, C. P. Romao, and D. M. Juraschek, *Phys. Rev. Lett.* **136**, 166801 (2026).
 - 34 D. M. Juraschek, R. M. Geilhufe, H. Zhu, M. Basini, P. Baum, A. Baydin, S. Chaudhary, M. Fechner, B. Flebus, G. Grissonanche, A. I. Kirilyuk, M. Lemesko, S. F. Maehrlein, M. Mignolet, S. Murakami, Q. Niu, U. Nowak, C. P. Romao, H. Rostami, T. Satoh, N. A. Spaldin, H. Ueda, and L. Zhang, *Nature Physics* **21**, 1532 (2025).
 - 35 S. Chaudhary, D. M. Juraschek, M. Rodriguez-Vega, and G. A. Fiete, *Physical Review B* **110**, 094401 (2024), pRB.
 - 36 A. von Hoegen, R. Mankowsky, M. Fechner, M. Forst, and A. Cavalleri, *Nature* **555**, 79 (2018).
 - 37 C. S. Davies, F. G. N. Fennema, A. Tsukamoto, I. Razdolski, A. V. Kimel, and A. Kirilyuk, *Nature* **628**, 540 (2024).
 - 38 M. Basini, M. Pancaldi, B. Wehinger, M. Udina, V. Unnikandanunni, T. Tadano, M. C. Hoffmann, A. V. Balatsky, and S. Bonetti, *Nature* **628**, 534 (2024).
 - 39 T. P. Martin and L. Genzel, *physica status solidi (b)* **61**, 493 (1974).
 - 40 D. M. Juraschek and S. F. Maehrlein, *Phys. Rev. B* **97**, 174302 (2018).